Experimental Determinations of Several Thermal Properties of a Mixture Containing 77 Mole % Propane in Methane

V. F. YESAVAGE, D. L. KATZ, and J. E. POWERS
Department of Chemical and Metallurgical Engineering, University of Michigan, Ann Arbor, Mich.

Results of experimental determinations are reported for a mixture containing approximately 77 mole % propane in methane. Measurements were made with both isobaric and throttling calorimeters in the liquid, critical, supercritical, gaseous, and two-phase regions in the temperature range from −240° to +300° F. at pressures between 100 and 2000 p.s.i.a. Data obtained in the single-phase region are summarized as tables of values of heat capacity, isothermal throttling coefficient, and Joule-Thomson coefficient. Experimental results for the enthalpy difference associated with a change of phase are reported for both isobaric and isothermal conditions. A skeleton enthalpy table based almost entirely on these experimental data is presented. Comparisons are made with other published calorimetric data.

ACCURATE calorimetric measurements of the effect of both temperature and pressure on the enthalpy of pure compounds and mixtures of known composition are useful for determination of a number of thermodynamic properties. They also serve to test the accuracy of values of thermal properties calculated from other thermodynamic data (mainly PVT data) and those estimated by various methods of prediction. This contribution presents calorimetric data for a binary mixture of methane and propane over appreciable ranges of temperature and pressure, establishes the probable accuracy of the data, and summarizes the results in the form of tabulated values of the enthalpy function.

Thermodynamic data for the pure components of the methane-propane binary are fairly extensive. Data for methane published prior to 1961 are summarized by Tester (*44*). Since that time extensive PVT data (*9, 16, 45, 46*) and results of calorimetric determinations (*5, 18, 19, 43*) have been reported for methane. Kuloor *et al.* (*21*) compiled data for propane published prior to 1956. Subsequently additional PVT (*8, 16*) and calorimetric data (*11, 15, 47, 48, 50*) for propane have been published.

Much less thermodynamic data have been reported for methane-propane mixtures. These include volumetric determinations (*16, 36, 42*), studies of phase behavior (*1, 34, 35, 36, 38, 40, 42*) and results of calorimetric measurements of the Joule-Thomson coefficient (*4, 14, 22, 51*), isobaric heat capacity and isobaric enthalpy change on vaporization (*22-25, 27, 31, 32, 51*), isothermal enthalpy differences (*7*), isothermal throttling coefficient (*25, 29, 51*), and heats of mixing of the pure liquids at low temperature (*6*).

The data presented in this report complement previously published data and include results of all types of calorimetric determinations listed above except direct measurements of the heat of mixing.

THERMODYNAMIC RELATIONS

The first law of thermodynamics applied to a flow calorimeter with negligible potential and kinetic energy effects operated at steady state with a pure component or mixture of constant composition reduces to:

$$(H_{T_2,P_2} - H_{T_1,P_1})_x = \frac{\dot{Q} - \dot{W}}{F} \tag{1}$$

In a properly designed flow calorimeter operated at a sufficiently high mass flow rate, the heat leak effects represented by $\dot{Q}$ in Equation 1 can be made negligible with respect to the other terms. This equation can then be applied to interpret data obtained by operation in the isobaric, isothermal, or isenthalpic modes.

Isobaric. Isobaric calorimeters are designed to have a very small pressure drop but to obtain precise results in terms of well defined thermodynamic properties it is necessary to correct the experimentally measured results for pressure drop as illustrated in Equation 2:

$$(H_{T_2} - H_{T_1})_{P_1,x} = -\frac{\dot{W}}{F} - \int_{P_1}^{P_2} \phi \, dP_{T_2,x} \tag{2}$$

where ϕ is the isothermal throttling coefficient defined by:

$$\phi = \left(\frac{\partial H}{\partial P}\right)_T \tag{3}$$

Equation 2 can be applied to determine enthalpy changes associated with isobaric vaporization of a mixture by using appropriate values of ϕ. Experimental data in terms of corrected isobaric enthalpy differences (Equation 2) are interpreted to yield values of the isobaric heat capacity, C_p, by application of the following integral relation in various forms:

$$(H_{T_2} - H_{T_1})_{P,x} = \int_{T_1}^{T_2} C_p dT_{P,x} \tag{4}$$

Isothermal. In making isothermal measurements a relatively large pressure drop is obtained within the calorimeter and electrical energy is added to the calorimeter to bring the outlet temperature as near to that of the inlet as is practical. To obtain precise results, a small correction is made, as indicated in Equation 5:

$$(H_{P_2} - H_{P_1})_{T_1} = -\frac{\dot{W}}{F} - \int_{T_1}^{T_2} C_p dT_{P_2} \tag{5}$$

Equation 5 can be applied to determine the enthalpy change resulting from isothermal vaporization of a mixture by using appropriate values of C_p. The data obtained in the single-phase region can be interpreted to yield point values of the isothermal throttling coefficient, ϕ, by application of the following integral equation:

$$(H_{P_2} - H_{P_1})_{T,x} = +\int_{P_1}^{P_2} \phi \, dP_{T,x} \tag{6}$$

The limitations of the recycle flow facility make it impractical to obtain data below a pressure of 100 p.s.i.a. To aid in determining enthalpy departures from zero pressure, values of ϕ were estimated at low pressures. The following equation was applied when using PVT data directly or making calculations based on an equation of state.

$$\phi = V - T\left(\frac{\partial V}{\partial T}\right)_{P,x} \tag{7}$$

PVT data at low pressures are conveniently summarized in terms of the second virial coefficient, B. This coefficient is related to the zero pressure value of the isothermal throttling coefficient, ϕ°, by the following expression:

$$\phi^\circ = B - T\left(\frac{dB}{dT}\right) \tag{8}$$

The second virial coefficient for mixtures, B_m, has the form:

$$B_m = x_1^2 B_{11} + 2x_1 x_2 B_{12} + x_2^2 B_{22} \tag{9}$$

and

$$\frac{dB_m}{dT} = x_1^2 \frac{dB_{11}}{dT} + 2x_1x_2 \frac{dB_{12}}{dT} + x_2^2 \frac{dB_{22}}{dT} \tag{10}$$

where B_{12} is a factor which takes into account the interactions of the binary pair.

Isenthalpic. When the properties of the fluid under investigation are such that a drop in pressure tends to result in an increase in temperature, it is not possible with the present equipment to adjust the outlet temperature to correspond to that of the inlet. Under such conditions, no electrical energy is added to the throttling calorimeter (except to the guard heater), and an isenthalpic change results.[1] Experimental results include the inlet and outlet temperatures and pressures. Interpretation of the results is complicated somewhat by the fact that with the throttling calorimeter used it is not convenient to vary the pressure drop over an appreciable range. Instead, experiments are made such that the inlet temperature is constant and the temperature rise is approximately equal for all values of the inlet pressure. Values of the integral-average Joule-Thomson coefficient, $\hat{\mu}$, over a pressure interval, $P_2 - P_1$, at the arithmetic average temperature can be estimated from results of this type by use of the expression:

$$\hat{\mu} = \left(\frac{T_2 - T_1}{P_2 - P_1}\right)_H \tag{11}$$

These average results can be used in conjunction with experimental values of $\hat{C}_p$ between the inlet and outlet temperatures to calculate the average isothermal throttling coefficient over the pressure interval, $P_2 - P_1$

$$\hat{\phi} = -\frac{\hat{C}_p}{\hat{\mu}} \tag{12}$$

The relation is exact and yields values of $\hat{\phi}$ at the inlet temperature.

The results obtained by application of Equation 12 can be used to determine point values of ϕ as a function of pressure. These results are then used in Equation 6 to determine isothermal enthalpy differences.

Thermodynamic Identity. In the area of experimental thermodynamics, mathematical identities are valuable in that they provide checks on the consistency of thermodynamic data. One example is the mathematical identity among the Joule-Thomson coefficient, μ, the isobaric heat capacity, C_p, and the isothermal throttling coefficient, ϕ, as given in the equation:

$$\mu C_p = -\phi \tag{13}$$

EXPERIMENTS

Equipment. The recycle-flow facility is illustrated in Figure 1. An A2CCV50/250 Corblin diaphragm compressor operates at essentially constant volumetric flow rate between constant inlet and outlet pressures. Variation in flow rate within the calorimeter section is provided for by a bypass line back to the compressor inlet buffer tank. The flow rate is determined using a Meriam laminar-flow meter located in the low pressure (100 p.s.i.a.) portion of the facility and maintained at constant temperature (27° C.). Storage tanks permit variation in the operating pressure in the calorimeter section.

The calorimeter section extends from the entrance to the cooling water coil through the hot oil bath. As two phases may exist in parts of this section, the various pieces of equipment are arranged vertically such that the flow is almost always downward. All other parts of the high-pressure portion of the facility are insulated, as indicated by the dashed lines, and are maintained at temperatures above the cricondentherm for the mixture to ensure that a single phase exists in all tubing and storage tanks outside the calorimeter section. The hot oil bath at the end of the calorimeter section provides for enough heat transfer to ensure that the exiting fluid is entirely vaporized under all conditions. The facility has been described in detail (*12, 18, 25, 30, 48*).

As indicated in Figure 1, two flow calorimeters are incorporated in the facility. The isobaric calorimeter uses electrical energy to increase the enthalpy of the flowing fluid (*12*). The throttling calorimeter uses a capillary tube with an insulated heating wire through its entire length to adjust the outlet temperature to that of the inlet (*25, 26, 28, 29*).

Under conditions such that an isenthalpic decrease in pressure results in an increase in temperature, this throttling

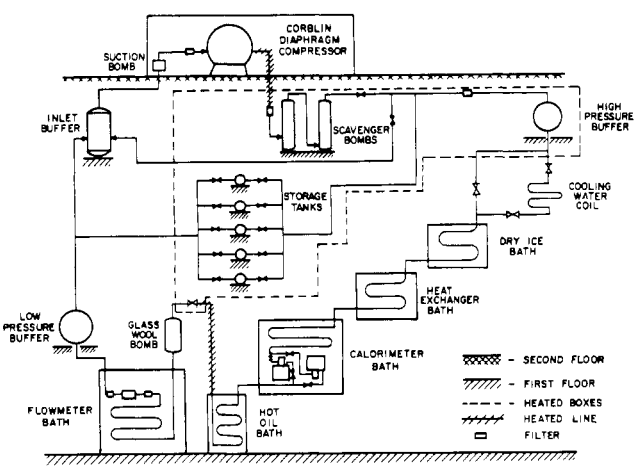

Figure 1. Flow diagram of modified recycle system

calorimeter is operated as a Joule-Thomson device (*48, 50*).

Procedure. In obtaining data, operating conditions are adjusted to establish desired values of inlet conditions of temperature and pressure and of flow rate and the power input is set at a desired value. Readings are taken and adjustments made as necessary until the condition of steady-state operation is obtained and maintained for at least 15 minutes. A single determination generally lasts from 1 to 2 hours, depending on the magnitude of the changes made between determinations.

Many of the measurements which are made are common for operation in all of the three modes, as indicated by Equation 1.

TEMPERATURE (T_1, T_2). The temperature at the inlet to the operating calorimeter is assumed to be equal to the temperature of the calorimeter bath, which is determined by a platinum resistance thermometer. Duplicate six-junction copper-constantan thermopiles were used in each calorimeter to determine temperature differences between the inlet and outlet. Both the resistance thermometer and the thermopiles were calibrated by the National Bureau of Standards. On the basis of these calibrations and the limitations in reading the potentials, it is estimated that the bath temperature is known within $\pm 0.01°$ F. or +0.05%, whichever is larger. When isothermal determinations are made at temperatures slightly greater than the cricondentherm the inlet fluid may be lower than that of the bath by as much as 0.1° F. and the error introduced in measuring the temperature difference may be as large as 0.05° F.

PRESSURE (P_1, P_2). The pressure at the inlet is determined by use of a Mansfield and Green pressure balance connected to the system by means of a Ruska differential pressure indicator. Considering the limits of calibration of the instrument and the possible effect of liquid in the leads it is estimated that the reported values of inlet pressure are accurate to ± 1 p.s.i.a. The slight pressure drop across the isobaric calorimeter is measured by means of a high-pressure mercury manometer to 0.1 inch. Whereas this may yield a relatively large percentage error in this determination at conditions of low pressure drop, such conditions also minimize the importance of this determination, as indicated by Equation 2. The pressure drop across the throttling calorimeter is determined using the differential pressure balance of Roebuck (*37*). The sensitivity of this instrument varies with pressure level, with a possible error of ± 1 p.s.i. at 2000 p.s.i.a. Thus the error in this determination is always 1% or less because pressure drops of less than 100 p.s.i.a. were not used.

COMPOSITION (x). A chromatograph incorporated as part of the recycle flow facility was used for frequent checks on the composition of the gas in the system. The chromatograph was calibrated with considerable care, using samples of known composition prepared by direct weighing. The chromatographic analyses are summarized in Figure 2. Although there is some variation in composition, especially when operating in or near the two-phase region, there is no indication of a change in average composition with time. It appears that the average composition is known to about ± 0.1 mole % or better.

The methane used in this investigation was donated by the Southern California Gas Co. The propane used was instrument grade as obtained from the Phillips Petroleum Co. Compositions of the mixture were determined by mass spectrometer and chromatographic analyses (Table I).

ELECTRICAL POWER ($\dot{W}$). The electrical energy addition to the calorimeter was furnished by a regulated power supply and the rate was determined by measuring the current flow and voltage drop using standard resistors and a K-3 potentiometer. Considering possible errors in both determinations, it is felt that values of $\dot{W}$ are accurate to $\pm 0.05\%$.

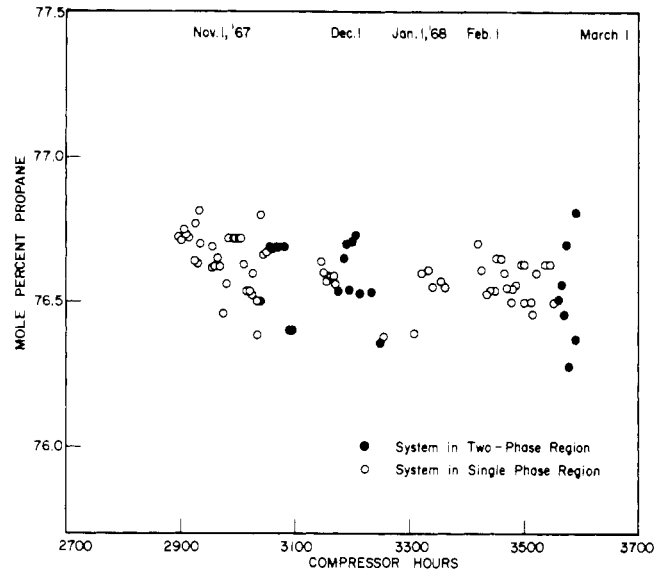

Figure 2. Composition of recycle gas during time of investigation

Table I. Composition of Nominal 77 Mole % Propane in Methane Mixture

	Chromatograph,[a] Mole %	Mass Spectrometer,[b] Mole %
Nitrogen	0.20	<0.05
Methane	23.16	24.23
Ethane	<0.05	<0.05
Carbon dioxide	<0.05	<0.05
Propane	76.53	75.77
Butane	0.11	<0.05
	<100.10	<100.20

[a] Sample taken from system in March 1968. [b] Sample taken from system in October 1967.

FLOW RATE (F). The rate at which the flowing gas passes through the calorimeter, F, is perhaps the most critical measurement in the determination of enthalpy differences by the use of flow calorimeters. A Meriam flowmeter was calibrated by collecting samples over a measured time interval and determining the mass by weighing. A set of calibration runs consists of approximately 10 such determinations at various flow rates. The flowmeter is operated at a nominal pressure of 80 p.s.i.g. at 27° C. The actual pressure is determined using a 180-inch mercury manometer. Density and viscosity corrections are made for variations of temperature, pressure, and composition. The results are interpreted using a correlation equation (*18*).

In an attempt to ensure the accuracy of the results, it is standard practice to calibrate the flowmeter with the mixture under study before any runs are made and after every 10 runs (approximately 50 data points) are complete. The first three calibrations made under these conditions were very successful and yielded reproducible results (lowest curve in Figure 3). All curves illustrate that the flow is not strictly laminar in the flowmeter; if it were, the results would lie on a horizontal line on this type of plot. The calibration data for the first three calibration runs lie essentially on a single line. The standard deviation of the experimental calibration points from the correlating equation for the 25 experimental points of these three runs is $\pm 0.20\%$.

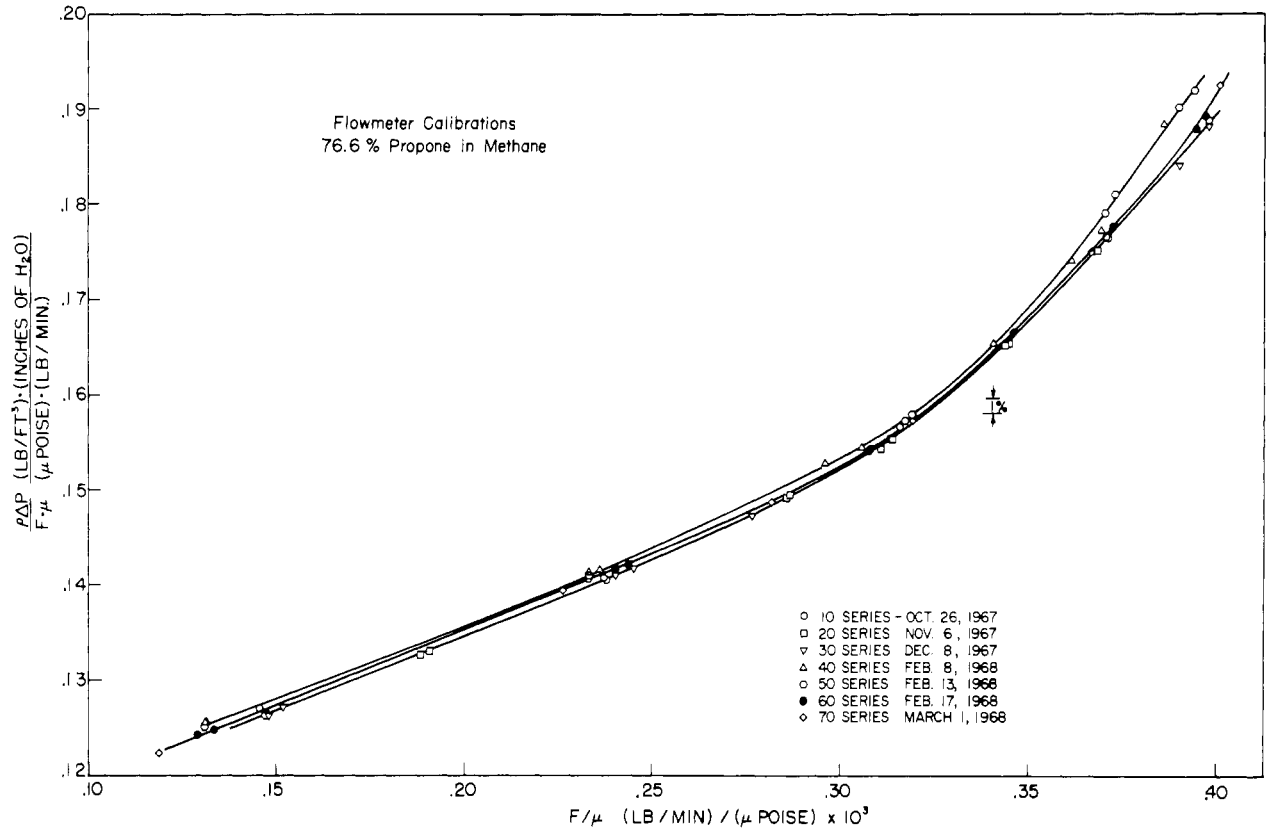

Figure 3. Flowmeter calibrations

The success of these early calibrations led to a deviation from standard practice and no recalibration was made between runs 20 and 46. During this interval of 9 weeks, the calibration changed. Calibrations were then made after run 46 and before run 49 (upper curve of Figure 3) and are fairly consistent (standard deviation as defined above for 20 calibration points of ±0.30%). Runs 47 and 48 are repeats of previous runs and were made in an attempt to establish when the flowmeter calibration changed.

Following the calibration after run 48, the flowmeter was removed from the system, cleaned ultrasonically, and recalibrated. Additional check runs were made to aid in the interpretation of the previous data and new data were obtained. Data from the last calibration which was made with this mixture agreed well with the one made subsequent to ultrasonic cleaning, as illustrated by the middle curve on Figure 3 (standard deviation of ±0.2%).

In using the results of flowmeter calibrations to establish the experimental values of the flow rate, results from the pair of calibration runs which bracket the experimental runs are usually used. The calibration runs used to interpret specific data for this mixture are indicated in Table II, together with values of the total number of points included in the calibration sets and the standard deviation of each set from the calibration equation.

CHECK ON ASSUMPTION OF ADIABATICITY. In applying Equation 1 to interpret experimental data, it is assumed that the calorimeter is adiabatic. It has been established for the isobaric mode (*33*) that this condition is satisfied if the heat capacity determined using the calorimeter is independent of the flow rate. Therefore, a series of isobaric determinations (runs 18 and 20) was made at four different flow rates to test the assumption of zero heat leakage. As illustrated in Figure 4, the heat capacity obtained is essentially independent of flow rate within the limits of precision of the measurements (±0.3%).

Isobaric measurements in the single-phase region are usually made in groups of four data points each. The inlet temperature is held constant and power input is adjusted to yield temperature rises of approximately 10°, 20°, 40°, and 80° F. In regions where C_p varies significantly with temperature (such as in the critical region) smaller temperature rises were investigated. Isobaric determinations through the two-phase region included determinations of

Table II. Calibration Data Used in Interpreting Experimental Results

Experimental Runs	Calibration Runs	No. of Calibration Points	Av. Dev., %
1-26 1R-3R	10,20,30	24	0.20
27-47	40,50	20	0.30
48-51 4R	60,70	16	0.21

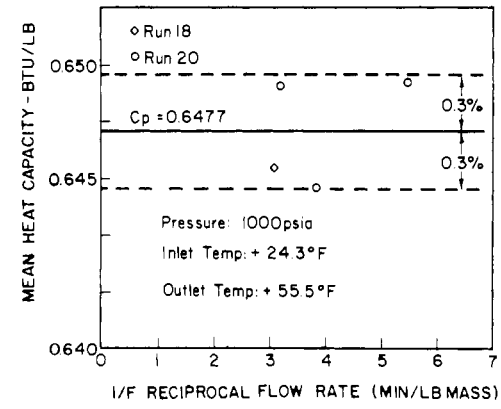

Figure 4. Check on adiabaticity of isobaric flow calorimeter

the heat capacity of the liquid and vapor at temperatures respectively below and above the saturation temperatures.

Isothermal determinations were made both in the single-phase region and across the two-phase region. The power input was adjusted until the outlet temperature was within 0.05° F. of the inlet temperature. In general, pressure drops between 100 and 500 p.s.i. were used.

Isenthalpic determinations were made at conditions of constant inlet temperature. For a given inlet pressure, the flow rate was adjusted to yield a pressure drop of about 200 p.s.i. at steady-state conditions. The inlet pressure was then adjusted to a new value and the process repeated until the entire single-phase region was covered. No isenthalpic determinations were made in the two-phase region. For each operating condition, no electrical energy was transferred to the throttling calorimeter. The radiation shield was heated to the temperature of the exiting fluid to provide guard heating, thereby reducing to a negligible value the heat transfer by radiation and conduction through the vacuum jacket.

Results. Experimental measurements of isobaric, isothermal, and isenthalpic changes in enthalpy for the mixture containing 76.6 mole % propane in methane have been presented in tabular form in progress reports to the Natural Gas Processors Association for the quarters ending December 31, 1967, and March 31, 1968, and are reported in final form in a thesis (*48*). Included are determinations in both the gaseous and liquid regions, as well as isobaric and isothermal traverses of the two-phase regions. The ranges of pressures and temperatures covered by these experiments are indicated by lines drawn on a PT diagram in Figure 5.

INTERPRETATION OF RESULTS

Isobaric. The isobaric data in the single-phase region were interpreted using Equation 2. The correction calculated from the integral term was almost always less than 1%. Typical results are shown as Figure 6, on which average values of heat capacity calculated from experimental results are plotted against temperature. Solid lines indicate basic results obtained in accordance with the procedure described previously and dashed lines are values obtained by difference from the basic results. A smoothed line is drawn through the data in accordance with Equation 4. Graphical procedures were used in establishing $C_p(T)$ in the vicinity of the peak and when extrapolation of data was required, but a majority of the data were processed by computer techniques (*48*). Figure 6 illustrates the broad maximum in the heat capacity which occurs in the region just above the critical point for the mixture. Although the variation in C_p at this pressure is significant (an increase by a factor of greater than 2 from 0° to 180° F.), this is much less of an increase than would be expected for a pure component at the same value of P/P_c where P_c is the true critical pressure of either the compound or of the mixture (about 925 p.s.i.a. for this mixture).

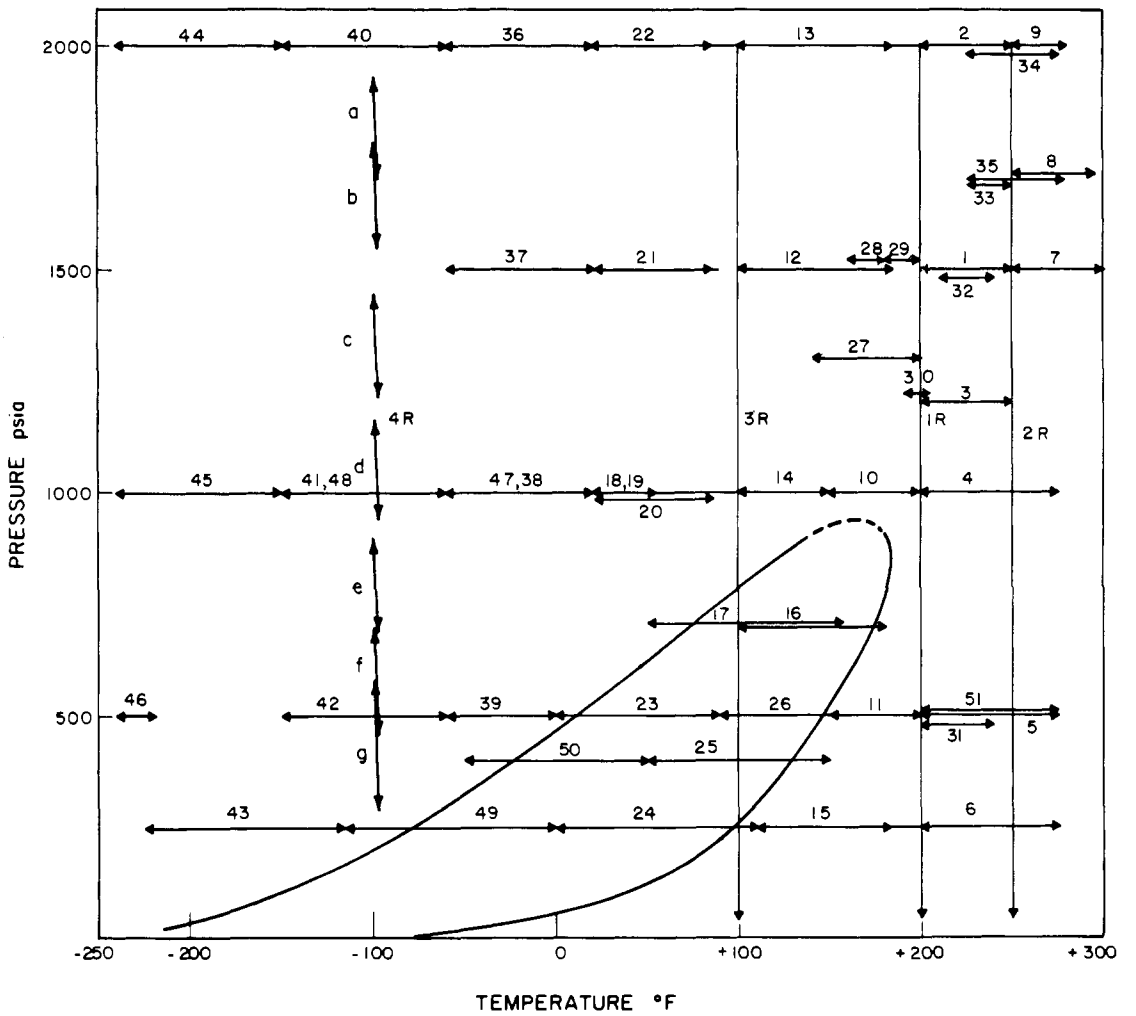

Figure 5. Pressures and temperatures of measurement

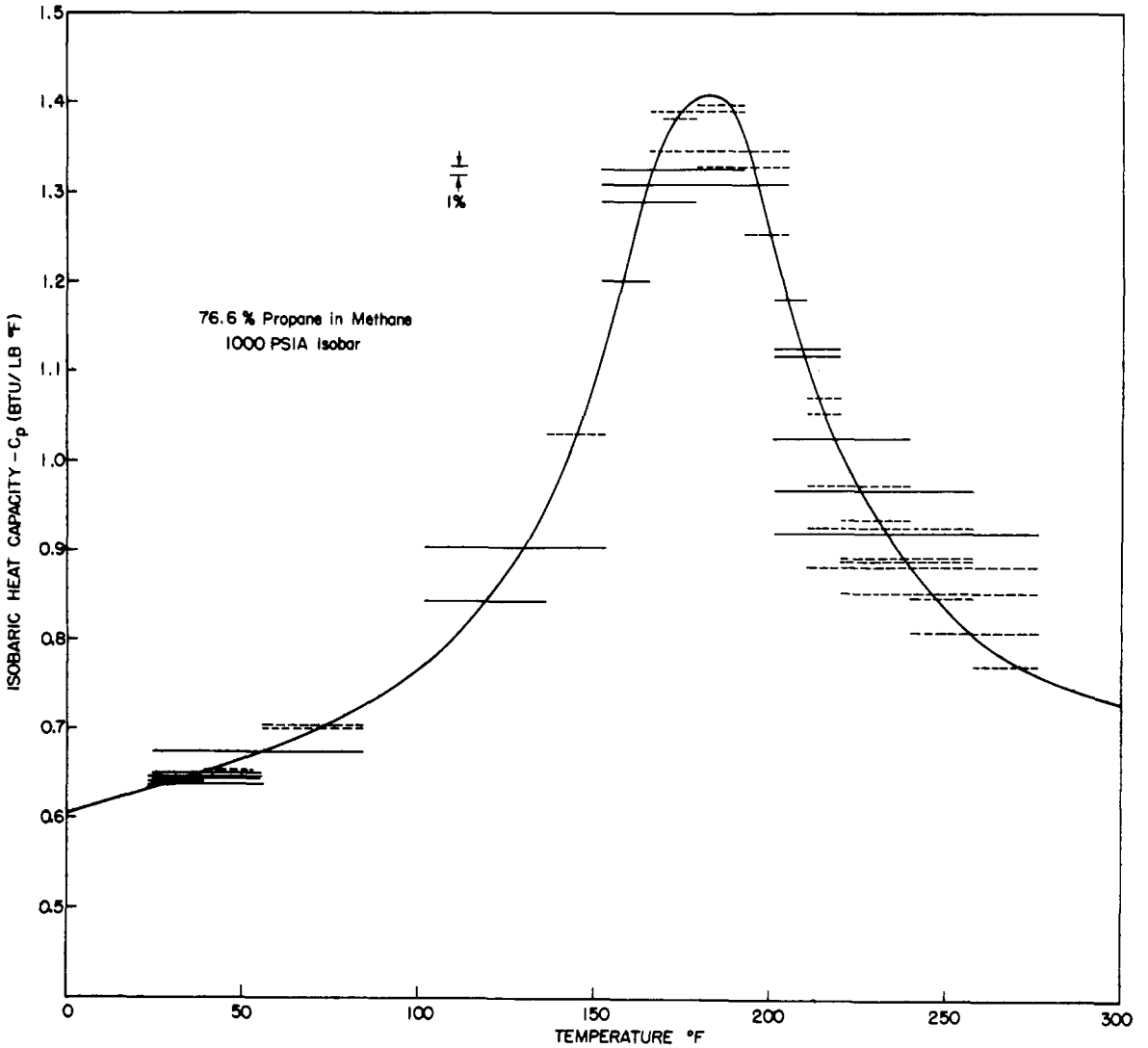

Figure 6. Isobaric heat capacity at 1000 p.s.i.a. in upper temperature range

A majority of the values of heat capacity, C_p, obtained from interpretation of isobaric data in the single-phase regions are summarized in Table III for equal intervals of temperature and pressure.

Significant changes in the value of the heat capacity occur not only in the region above the critical point for the mixture but also near the two-phase locus. Figure 7 illustrates typical values of experimental data, with the smoothed curve through the data representing values of the heat capacity near the two-phase region. Table IV lists values of heat capacity in the regions of significant change, such as near the maxima in the heat capacity and near the saturation curves.

A typical enthalpy traverse of the two-phase region at constant pressure is illustrated in Figure 8. The traverse was made as two runs: Run 17 had an inlet temperature of about 50° F. and was terminated within the two-phase region at about 140° F. In run 16 a two-phase mixture at about 100° F. was fed to the calorimeter and the run was terminated after the exiting fluid was totally vaporized at about 190° F. The results of the two runs are consistent in the region of overlap, as illustrated in Figure 8. This procedure was followed so that enthalpy traverses could be made across the two-phase regions at larger flow rates than would be possible if the entire change were experienced in one run. This results from a limitation on the rate at which energy can be added to the flowing fluid without burning out the heating element.

The isobaric enthalpy change on vaporization was determined from such data by establishing the bubble and dew points at the discontinuity in slope of the curve. Experimentally determined values of the isobaric enthalpy change on vaporization are listed in Table V together with the experimentally determined values of the bubble point and the dew point for the mixture.

Isothermal. The isothermal data obtained in the single-phase region were interpreted in accordance with Equation 6 and plots made of the average value of the isothermal throttling coefficient as a function of pressure. Typical results are shown in Figure 9. A maximum exists in the curve, as the data were obtained at a temperature just above the two-phase region (run 1R, Figure 5).

As the lower limit on pressure is about 100 p.s.i.a., it was necessary to estimate $\phi = f(P)$ at low pressures. To aid in this estimation, values were calculated using the BWR equation of state with the original constants for methane and propane (*2*) together with mixing rules as originally suggested (*3*). Typical results are presented as a center line on Figure 9. In addition, Equations 9 to 11 were used with published values of the second virial coefficient for methane and propane and the interaction term (*17*) to estimate $\phi°$. The resulting value at 201° F. is plotted on Figure 9. As another check, PVT data for the mixture (*36*) as interpreted (*10*) using Equations 7 and 8 yielded values of $[(H° - H)/\Delta P]_T$ between zero pressure and 200 p.s.i.a. A typical value is presented as

Table III. Tabulated Values of Isobaric Heat Capacities for a Nominal 77 Mole % Propane in Methane Mixture

Temp.,	C_p, B.t.u./Lb.-° F. Pressure, P.S.I.A.					
° F.	0	250	500	1000	1500	2000
−280	0.485[a]	0.490	0.492	0.492	0.486	0.484
−270	0.487[a]		0.493	0.494	0.488	0.486
−260	0.489[a]	0.493	0.495	0.495	0.489	0.487
−250			0.497	0.496	0.491	0.490
−240		0.496	0.499	0.498	0.494	0.493
−230		0.498	0.501	0.500	0.497	0.495
−220		0.501	0.504	0.502	0.500	0.499
−210		0.503	0.506	0.504		0.501
−200		0.507	0.509	0.506	0.504	0.504
−190		0.510	0.512	0.509		0.506
−180		0.513	0.515	0.511	0.508	0.508
−170		0.517	0.518	0.513		0.510
−160		0.521	0.521	0.515	0.512	0.512
−150		0.525	0.524	0.518		0.514
−140		0.529	0.527	0.522	0.520	0.517
−130		0.533	0.533	0.527		0.520
−120		0.538	0.534	0.532	0.528	0.523
−110		0.543	0.538	0.537		0.527
−100		0.549	0.542	0.542	0.538	0.531
−90		0.555	0.546	0.546		0.535
−80		0.561	0.551	0.550	0.545	0.540
−70			0.557	0.555		0.546
−60			0.564	0.559	0.553	0.551
−50			0.572	0.564	0.558	0.557
−40			0.580	0.570	0.565	0.563
−30			0.588	0.576	0.571	0.569
−20			0.597	0.584	0.577	0.576
−10			0.607	0.593	0.584	0.583
0			0.617	0.604	0.592	0.591
10				0.616	0.601	0.597
20				0.628	0.611	0.604
30				0.640	0.621	0.611
40				0.652	0.630	0.619
50				0.665	0.642	0.627
60				0.680	0.653	0.636
70				0.696	0.664	0.645
80				0.716	0.676	0.655
90				0.738	0.689	0.665
100	0.425[b]	0.601		0.766	0.704	0.676
110	0.431[b]	0.567		0.801	0.721	0.687
120	0.437[b]	0.541		0.847	0.744	0.700
130	0.443[b]	0.530		0.904	0.768	0.714
140	0.449[b]	0.525		0.980	0.794	0.728
150	0.455[b]	0.523	0.738	1.088	0.819	0.743
160	0.461[b]	0.523	0.718	1.233	0.845	0.758
170	0.467[b]	0.523	0.679	1.360	0.870	0.773
180	0.473[b]	0.523	0.652	1.407	0.899	0.786
190	0.479[b]	0.525	0.633	1.388	0.922	0.800
200	0.485[b]	0.528	0.621	1.259	0.948	0.813
210	0.491[b]	0.531	0.613	1.115	0.976	0.827
220	0.497[b]	0.535	0.608	1.011	1.001	0.840
230	0.503[b]	0.539	0.603	0.940	1.002	0.854
240	0.509[b]	0.544	0.601	0.884	0.984	0.868
250	0.514[b]	0.548	0.601	0.839	0.960	0.881
260	0.520[b]	0.553	0.602	0.801	0.940	0.886
270	0.526[b]	0.559	0.604	0.776	0.916	0.875
280	0.532[b]	0.565	0.606	0.756	0.896	0.855
290	0.538[b]	0.571	0.609	0.741	0.879	0.834
300	0.543[b]	0.577	0.612	0.729	0.864	0.812

[a] Experimental data of Cutler and Morrison (*6*). [b] Ideal gas values of Rossini *et al.* (*39*).

a dashed line on Figure 9. A solid line (such as shown on Figure 9) was drawn to be consistent with the data obtained at elevated pressures and the estimates based on data from the literature in the low pressure range. Values of the isothermal throttling coefficient, ϕ, obtained by interpreting the data (including values of $\phi°$ established

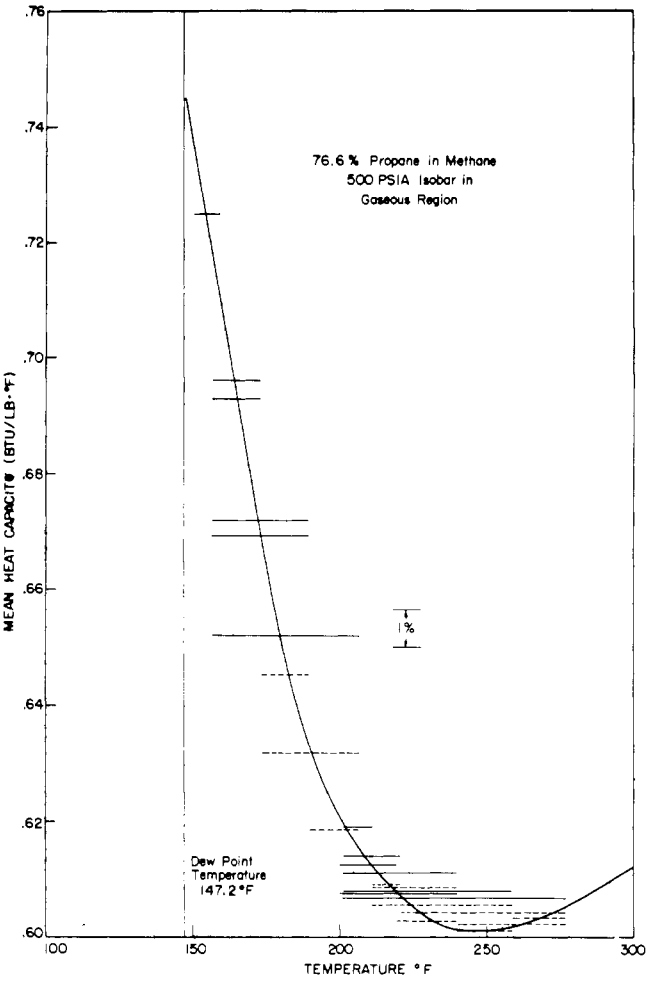

Figure 7. Isobaric heat capacity at 500 p.s.i.a. illustrating variation in value near the two-phase region

as outlined above) are reported for each of the experimental isotherms in Table VI.

One experimental isothermal run was made across the two-phase region (Figure 10). Breaks in the curve indicate both the upper pressure at which vaporization started and the lower pressure at which vaporization was complete.

Isenthalpic. Seven determinations were made with the throttling calorimeter under conditions such that a drop in pressure resulted in an increase in temperature (run 4R on Figure 5). The inlet temperature was constant at −96.8° F. in all cases. The data were interpreted in accordance with Equation 11 as described in detail elsewhere (*48*). Values of the Joule-Thomson coefficient at the arithmetic average temperature −96.2° F. are listed at various pressures in Table VII.

As indicated by Equation 12, the isenthalpic results were used together with integral C_p values to obtain integral average values of the isothermal throttling coefficient. These results are shown on Figure 11 and were interpreted to determine the point values of the isothermal throttling coefficient, ϕ, at −96.8° F. as listed in Table VI.

Consistency Checks. If isobaric, isothermal, and isenthalpic data are obtained for a system at properly selected values of pressure and temperature, it is possible to check the thermodynamic consistency of these data. The principle of this type of check is illustrated with reference to Figure 12. Consider the closed loop between 99.9° and 201° F. and between 500 and 1000 p.s.i.a. Using Equation 4 and the data summarized in Figure 6 a value for the enthalpy difference at 1000 p.s.i.a. between 99.9° and 201.0° F. was determined to be +111.6 B.t.u. per pound (the sign is

Table IV. Supplemental Table of Experimental Values of Isobaric Heat Capacity, C_p (B.t.u./Lb. ° F.)

Pressure, P.S.I.A.										
					Temperature, ° F.					
400	−45	−40	−35	−30	−25	−24.0	131.2	135	140	145
					C_p, B.t.u./Lb. ° F.					
	0.579	0.586	0.594	0.601	0.609	0.610	0.736	0.701	0.655	0.610
					Temperature, ° F.					
700	50	55	60	65	70	75	170.1	175	180	185
					C_p, B.t.u./Lb. ° F.					
	0.678	0.688	0.698	0.708	0.719	0.729	1.276	1.153	1.028	0.906
					Temperature, ° F.					
1200	190	200	210	220	230	240	245	250	255	260
					C_p, B.t.u./Lb. ° F.					
	1.169	1.166	1.153	1.118	1.061	0.983	0.943	0.903	0.834	0.764
					Temperature, ° F.					
1700	220	225	230	235	240	245	250	260	270	280
					C_p, B.t.u./Lb. ° F.					
	0.915	0.925	0.933	0.937	0.936	0.933	0.927	0.915	0.901	0.889

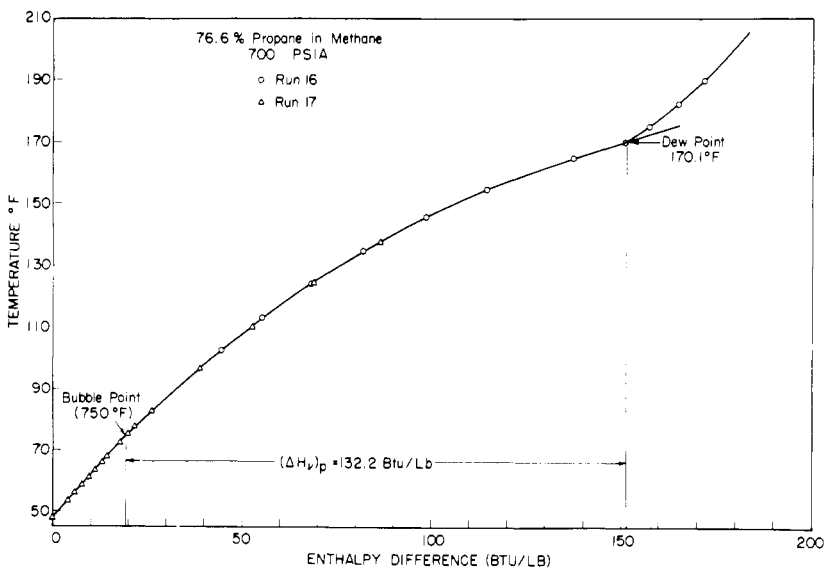

Figure 8. Isobaric enthalpy traverse through two-phase region at 700 p.s.i.a.

Table V. Properties of Nominal 77 Mole % Propane in Methane Mixture at Phase Boundaries

Pressure, P.S.I.A.	Temperature, ° F. Bubble point	Dew point	$(\Delta H_{vap})_P$, B.t.u./Lb.
250	−81.0	95.7	232.1
400	−24.0	131.2	208.0
500	12.2	147.0	183.2
700	75.0	170.1	132.2

associated with a clockwise path). Similarly an enthalpy difference of −138.97 B.t.u. per pound was established between the same two temperatures at 500 p.s.i.a. using data summarized in Figures 7 and 8. Applying Equation 6 plus data summarized in Figure 9 yielded a value of +48.47 B.t.u. per pound at 201.0° F. between 1000 and 500 p.s.i.a. The loop was closed by using the data of Figure 10 to determine the enthalpy difference at 99.9° F. between 500 and 1000 p.s.i.a. to be −22.0 B.t.u. per pound. Two of these legs involved data obtained within the two-phase region. The algebraic sum of these enthalpy differences is not identically equal to zero as required by the property relation but has a value of −0.89 B.t.u. per pound as indicated on Figure 12. For this particular loop, the percentage deviation, defined by

$$\text{Percentage deviation} \equiv \frac{\sum_i \Delta H_i}{\sum_i |\Delta H_i|} \times 100 \qquad (14)$$

is equal to −0.28%. This particular consistency check is one of the more severe tests of the data, because results are included just above both the critical point and the cricondentherm and within the two-phase region.

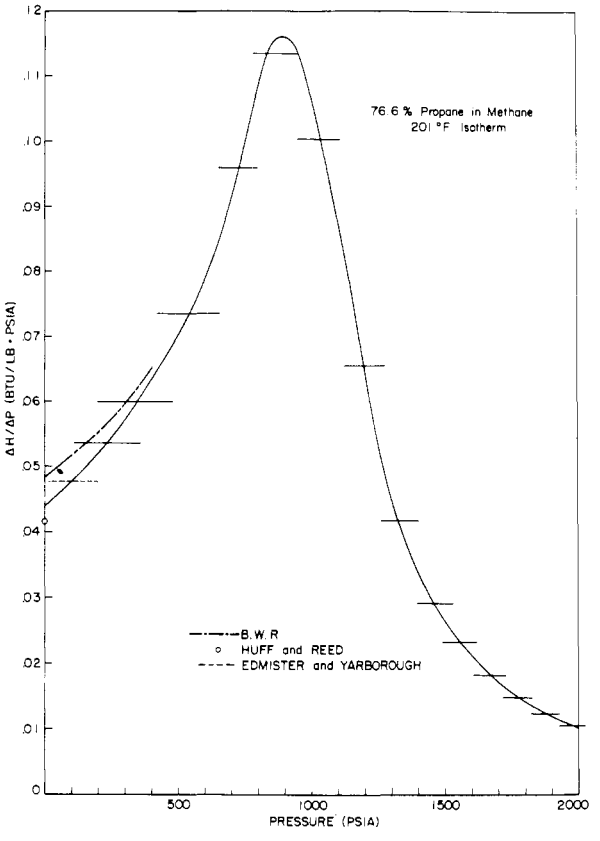

Figure 9. Isothermal throttling coefficient at 201° F.

Table VI. Experimental Values of Isothermal Throttling Coefficient, ϕ, for Nominal 77 Mole % Propane in Methane Mixture

[$\phi \times 10^2$ (B.t.u./lb. p.s.i.a.)]

Pressure, P.S.I.A	Temperature, ° F.			
	−96.8[a]	99.9	201.0	251.0
0[b]	...	...	−4.39	−3.76
100	...	...	−4.76	−4.03
200	...	...	−5.19	−4.30
300	+0.301	...	−5.70	−4.56
400	+0.302	...	−6.33	−4.83
500	+0.303	...	−7.01	−5.11
600	+0.304	...	−7.86	−5.43
700	+0.304	...	−9.13	−5.79
800	+0.305	−0.734	−10.81	−6.81
900	+0.306	−0.596	−11.60	−6.58
1000	+0.307	−0.483	−10.66	−6.77
1100	+0.308	−0.396	−8.77	−6.70
1200	+0.308	−0.325	−6.45	−6.36
1300	+0.309	−0.265	−4.54	−5.89
1400	+0.310	−0.214	−3.39	−5.16
1500	+0.311	−0.170	−2.62	−4.39
1600	+0.313	−0.130	−2.10	−3.70
1700	+0.316	−0.101	−1.72	−3.05
1800	+0.319	−0.071	−1.42	−2.53
1900	+0.328	−0.044	−1.19	−2.22
2000	+0.339	−0.017	−1.00	−1.98

[a] Calculated using Equation 13. [b] Extrapolation to zero pressure based primarily on PVT data

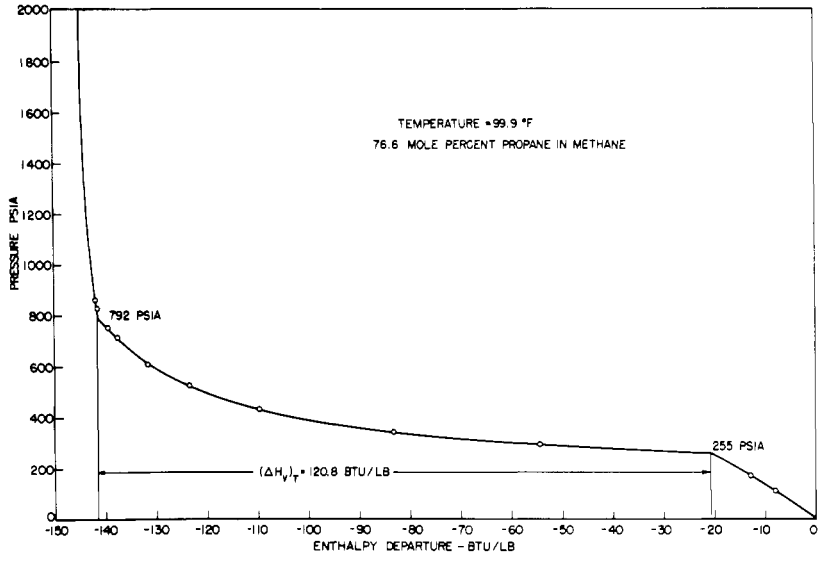

Figure 10. Isothermal enthalpy traverse through two-phase region at 100° F.

Figure 12 summarizes the results of all of the consistency checks made with the data obtained for this system. Values are presented only for the smallest loops, as bigger loops will usually yield a value for percentage deviation that is smaller than the largest included within the constituent smaller loops. As can be seen, the largest percentage deviation is 0.47% for a loop which includes both isobaric and isothermal data within the two-phase region. The average absolute deviation for the 14 loops was found to be 0.18%. This should give some indication of the accuracy of the data presented.

Table VII. Experimental Values of Joule-Thomson Coefficient, μ, at −96.2° F., for Nominal 77 Mole % Propane in Methane Mixture

Pressure, P.S.I.A.	$-\mu \times 10^3$ ° F./P.S.I.	Pressure, P.S.I.A.	$-\mu \times 10^3$, ° F./P.S.I.
300	5.50	1200	5.72
400	5.52	1400	5.78
600	5.57	1600	5.85
800	5.62	1800	6.02
1000	5.67		

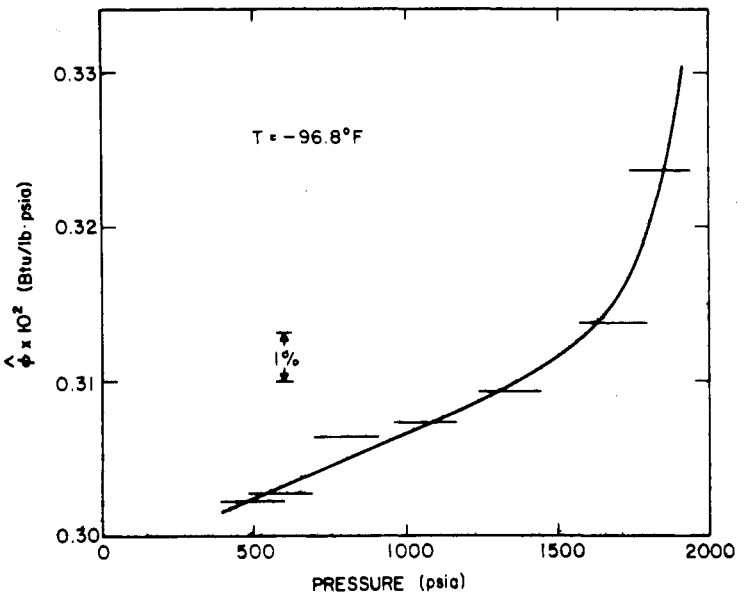

Figure 11. Values of the integral-average isothermal throttling coefficient, $\hat{\phi}$, at −96.8° F. calculated from experimental values of $\hat{\mu}$ and $\hat{C}_p$

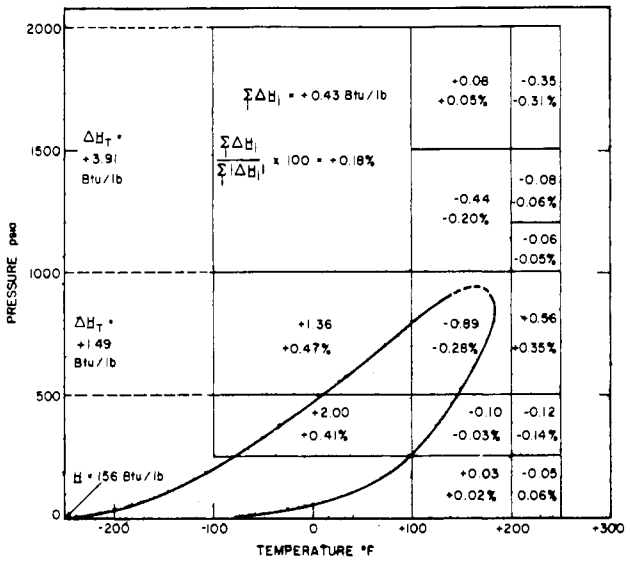

Figure 12. Summary of consistency checks

Table VIII. Tabulated Values of Enthalpy for Nominal 77 Mole % Propane in Methane Mixture

Pressure, P.S.I.A.	Temperature, ° F. Bubble point	Temperature, ° F. Dew point	Saturated Liquid Enthalpy, B.t.u./Lb.	Saturated Vapor Enthalpy, B.t.u./Lb.	Latent Heat of Vaporization B.t.u./Lb.
100	−144	+36	69.0	325.0	256.0
200	−100	+83	93.6	335.7	242.1
300	−62	+110	115.3	342.6	227.3
400	−24	+132	137.2	344.7	207.5
500	12	147	159.2	342.7	183.5
600	47	160	181.3	338.7	157.4
700	76	170	201.6	333.4	131.8
800	102	178	221.6	326.5	104.9

H, B.t.u./Lb.

Temp., ° F.	Pressure, P.S.I.A. 0	250	500	750	1000	1250	1500	1750	2000
−280	234.9	1.2	2.1	3.1	4.2	5.2	5.9	6.9	8.0
−270	237.7	6.1	7.1	8.2	9.2	10.0	10.7	11.6	12.9
−260	240.4	11.1	12.0	13.3	14.2	15.0	15.6	16.5	17.8
−250	243.1	16.1	17.1	18.3	19.2	20.0	20.5	21.4	22.7
−240	245.9	21.1	22.0	23.2	24.0	24.9	25.5	26.5	27.7
−230	248.6	26.0	27.0	28.2	29.0	30.0	30.7	31.6	32.6
−220	251.4	30.9	32.1	33.2	34.0	34.9	35.7	36.5	37.6
−210	254.2	35.9	37.0	38.1	39.0	39.9	40.7	41.5	42.6
−200	257.1	40.9	42.0	43.2	44.0	44.9	45.8	46.6	47.6
−190	259.9	45.9	47.1	48.4	49.2	50.0	50.8	51.5	52.6
−180	262.8	50.9	52.3	53.5	54.4	55.2	55.9	56.7	57.6
−170	265.7	56.1	57.5	58.5	59.4	60.4	61.0	61.9	62.7
−160	268.7	61.3	62.7	63.8	64.6	65.5	66.1	67.0	67.8
−150	271.7	66.6	68.0	67.0	69.8	70.6	71.4	72.2	73.0
−140	274.7	71.8	73.2	74.2	75.0	75.7	76.6	77.4	78.2
−130	277.7	77.0	78.5	79.4	80.2	80.8	81.7	82.5	83.3
−120	280.8	82.3	83.8	84.8	85.5	86.0	86.9	87.6	88.4
−110	284.0	87.9	89.0	90.2	90.8	91.5	92.3	93.0	93.6
−100	287.1	93.7	94.4	95.5	96.2	97.0	97.7	98.4	98.9
−96.8	288.2	95.7	96.1	97.2	98.0	98.6	99.3	100.0	100.5
−90	290.4	99.4	100.0	100.9	101.6	102.2	103.0	103.6	104.2
−80	293.6	105.0	105.5	106.3	107.0	107.6	108.3	109.0	109.5
−70	296.9	112.3	111.0	111.9	112.5	113.0	113.7	114.5	114.9
−60	300.3	119.3	116.7	117.4	118.0	118.6	119.5	120.1	120.4

(Continued)

ENTHALPY DIAGRAM

The data reported above have been used to prepare a skeleton table of values of the enthalpy of this mixture at selected values of pressure and temperature (Table VIII). In addition a *PTH* diagram has been prepared (*49*).

The following procedure was used in preparing the skeleton table and the diagram:

Reference states were taken to be $H = 0$ B.t.u. per pound for the pure components as saturated liquids at −280° F. This choice is consistent with that previously used for pure methane (*18, 19*), pure propane (*48, 50, 52*) and other mixtures of propane and methane which have been investigated (*22-25, 27, 31, 32*).

The enthalpy of pure methane as a gas at zero pressure and +201.0° F. was calculated using published data on the latent heat of vaporization at 5 p.s.i.a. (*13*), the BWR equation of state with the original constants (*2*) to correct from 5 p.s.i.a. to zero pressure at −280° F., and published values of the ideal gas heat capacity (*39*) between −280° and +201.0° F. These calculations are summarized below:

	H, B.t.u./Lb.
Enthalpy change on vaporization at −280° F.	+228.27
Effect of pressure on enthalpy (5 to 0 p.s.i.a.)	+1.43
Effect of temperature on zero pressure enthalpy (−280° to +201.0° F.)	+248.67
$H^{\circ}_{C_1}$ (pure methane at zero pressure and +201.0° F.)	+478.37

The enthalpy of pure propane as a gas at zero pressure and 201.0° F. was calculated using data on the liquid phase heat capacity (*20*), the latent heat of vaporization at 1 atm. (*20*), the BWR equation of state (*2*) to correct from 1 atm. to zero pressure at the normal boiling point, and values of the ideal gas heat capacity (*39*) to account for a change in temperature from the normal boiling point of propane to 201.0° F. These calculations are summarized below:

	H, B.t.u./Lb.
Saturated liquid (−280 to −43.7° F.)	115.30
Enthalpy change on vaporization at −43.7° F.	183.17
Effect of pressure on enthalpy (14.7 to 0 p.s.i.a.)	2.70
Effect of temperature on zero pressure enthalpy (−43.7° to +201.0° F.)	97.99
$H^{\circ}_{C_3}$ (pure propane at zero pressure and +201.0° F.)	399.16

The enthalpy of the propane-methane mixture at zero pressure and 201.0° F. was calculated assuming negligible heat of mixing under these conditions. The molecular weight of methane was taken to be 16.042 and that of propane as 44.094. The resulting value for the mixture is 407.08 B.t.u. per pound.

The isothermal effect of pressure on the enthalpy of the mixture at 201.0° F. was established from the basic experimental data obtained at this temperature (see Figure

Table VIII. *Continued*

Temp., ° F.	H, B.t.u./Lb. Pressure, P.S.I.A.								
	0	250	500	750	1000	1250	1500	1750	2000
−50	303.7	126.5	122.4	123.0	123.6	124.4	125.1	125.7	125.9
−40	307.1	133.8	128.2	128.6	129.3	130.1	130.8	131.3	131.4
−30	310.6	140.9	134.0	134.3	134.9	135.7	136.4	136.9	137.1
−20	314.2	148.2	139.9	140.1	140.6	141.4	142.2	142.8	143.0
−10	317.8	156.2	145.8	146.0	146.3	147.1	148.0	148.5	148.8
0	321.4	163.7	152.0	152.1	152.1	152.9	153.9	154.3	154.7
10	325.2	172.5	158.3	158.2	158.3	159.0	159.9	160.3	160.7
20	328.9	181.2	165.0	164.4	164.5	165.2	165.9	166.4	166.8
30	332.7	191.1	173.1	170.6	170.7	171.5	172.0	172.6	173.0
40	336.6	201.8	181.4	176.9	177.3	177.9	178.4	178.7	179.0
50	340.5	214.7	189.7	183.4	183.9	184.4	184.9	185.0	185.1
60	344.5	229.4	198.8	190.5	190.8	191.0	191.4	191.5	191.4
70	348.6	249.1	207.9	197.6	197.7	197.8	197.9	197.9	197.8
80	352.7	276.2	218.1	204.8	204.6	204.9	204.5	204.4	204.2
90	356.9	312.0	228.6	212.3	212.0	211.7	211.4	211.0	210.7
100	361.1	340.7	240.5	221.9	219.3	218.7	218.3	217.7	217.5
110	365.4	346.9	254.2	231.6	227.2	226.0	225.4	224.8	224.2
120	369.7	352.3	271.1	242.0	235.4	233.9	233.0	232.0	231.2
130	374.1	357.5	292.0	253.4	243.6	241.9	240.6	239.5	238.3
140	378.6	362.8	317.0	266.5	253.4	250.3	248.4	246.9	245.5
150	383.1	368.1	345.0	281.5	263.6	259.6	256.4	254.3	253.0
160	387.7	373.3	352.6	299.0	275.1	268.9	264.5	262.0	260.5
170	392.3	378.5	359.2	318.8	288.2	278.9	273.0	269.6	268.1
180	397.0	383.8	366.0	337.7	302.6	288.9	282.0	278.3	276.0
190	401.8	389.1	372.6	347.7	316.1	298.8	291.0	286.7	283.8
200	406.6	394.2	378.7	356.6	329.5	309.0	300.0	295.0	291.9
201.0	407.1	394.8	379.4	357.5	330.7	310.2	301.0	295.8	292.8
210	411.5	399.6	384.8	365.1	341.2	320.3	309.4	303.6	300.2
220	416.4	404.9	391.0	372.8	351.5	331.5	319.4	312.9	308.8
230	421.4	410.3	397.0	380.5	361.4	342.2	329.4	322.1	317.3
240	426.4	415.7	403.0	387.9	370.6	352.7	339.6	331.3	326.0
250	431.5	421.3	409.0	395.2	378.9	362.6	349.4	340.1	334.7
251.0	432.0	421.9	409.8	396.1	379.8	363.6	350.3	341.2	335.6
260	436.7	426.7	415.0	402.0	387.2	372.4	359.2	349.6	343.4
270	441.9	432.2	421.2	408.7	395.0	381.0	368.0	358.3	352.2
280	447.2	437.7	427.3	415.4	402.4	389.0	376.9	367.9	360.8
290	452.5	443.5	433.2	431.6	409.4	397.2	385.8	376.8	369.3
300	457.9	449.3	440.2	427.7	416.0	404.8	394.5	385.6	377.6

9). As indicated previously, extrapolation of the experimental data to zero pressure was necessary and involved application of data from the literature (*2, 3, 10, 17, 36*).

Isobaric data reported here were used at various pressures to determine the isobaric effect of temperature on enthalpy in both the gaseous and liquid regions as well as within the two-phase envelope. The limits of the two-phase region were determined using results from the traverses of the two-phase regions which were made during this investigation (Table V and Figure 8) supplemented by data from the literature (*1, 35, 36, 38, 40, 42*).

A skeleton table of values determined in this manner was prepared. Slight adjustments were made in the values, such that all deviations reported in Figure 12 were reduced to zero. The final results are presented as Table VIII.

Values from the skeleton table were plotted on graph paper and a smooth plot of the results was prepared by graphical methods. The *PTH* diagram is presented elsewhere (*49*).

COMPARISON WITH OTHER PUBLISHED DATA

Enthalpy. Very few data reported in the literature permit direct comparison with the data reported here. Cutler and Morrison (*6*) report data on the heat capacity of liquid mixtures of methane and propane at temperatures around −280° F. as well as data on the heat of mixing of liquid methane and propane at −280° F. Although these temperatures are somewhat lower than any used in this investigation (lower limit ≅ −240° F.) the values of C_p from the two investigations are consistent, as has been illustrated (*49*). A very excellent agreement was obtained when the value of the enthalpy change on mixing, ΔH^M at −250° F. obtained by extrapolation from −262° F. of the data of Cutler and Morrison (+15.36 B.t.u. per pound) was compared with −250° F. calculated from results of the present investigation and data for pure methane and pure propane as reported in the literature (+15.6 B.t.u. per pound). Details are presented elsewhere (*49*).

Values of C_p at zero pressure for the mixture calculated from published values for the pure components (*39*) are consistent with the values of C_p obtained during this investigation at pressures of 250 p.s.i.a. and higher. Details have been presented (*49*).

Data on the Joule-Thomson coefficient, μ, have been published for propane (*41*) and several binary mixtures of methane and propane (*4*). The values of μ for propane can be extended to elevated pressures by applying Equation 13 with published values of C_p and ϕ (*50*). These values were interpolated with respect to composition to establish the values reported in Table IX, which also lists values of C_p and ϕ from this investigation together with calculated values of $\mu = -\phi/C_p$ and the ratio $-\mu\ C_p/\phi = 1.00$. The interpolated values of μ are consistent with experimental results of this investigation to ±2%.

Table IX. Test of Consistency of Data Based on Equation 13

Temp., °F.	Pressure, P.S.I.A.	C_p, B.t.u./ Lb. °F.	ϕ, B.t.u./ Lb. P.S.I.	$-\phi/C_p$, °F./ P.S.I.	μ, °F./ P.S.I.	$-\mu C_p/\phi$
	0	0.486	−0.0438	0.0901	...	...
201	200	0.517	−0.0519	0.1039	0.1034[a]	0.995
	400	0.579	−0.0633	0.1093	0.1115[a]	1.02
	0	0.514	−0.0376	0.0732	...	...
250	200	0.541	−0.0430	0.0795	0.0807[b]	1.015
	400	0.577	−0.0483	0.0837	0.0837[b]	1.000
	600	0.631	−0.0543	0.0861	0.0874[b]	1.016
	800	0.705	−0.0618	0.0877	0.0874[b]	0.997

[a] Interpolated with respect to composition using values of μ for propane from (*41*) and for methane-propane mixtures from (*4*). [b] Interpolated with respect to composition using values of μ for methane-propane mixtures from (*4*) and values of μ for propane calculated using Equation 13 and data for C_p and ϕ from (*50*).

ACKNOWLEDGMENT

The authors thank A. W. Furtado, J. C. Golba, and J. Boissonneault for their substantial part in obtaining the experimental data. (The National Bureau of Standards provided a number of essential calibrations.) Mr. Golba was supported by a grant from the American Petroleum Institute.

NOMENCLATURE

- B = second virial coefficient, cu. ft./lb. mole
- B_{11}, B_{22} = second virial coefficient for pure components 1 and 2, cu. ft./lb. mole
- B_{12} = second virial interaction parameter for a mixture of components 1 and 2, cu. ft./lb. mole
- C_p = heat capacity at constant pressure, B.t.u./lb. ° F.
- F = mass flow rate, lb./min.
- H = specific enthalpy, B.t.u./lb.
- P = pressure, p.s.i.a.
- $\dot{Q}$ = rate of heat transfer, B.t.u./min.
- T = temperature, ° R.
- x = mole fraction
- $\dot{W}$ = rate of electrical energy transfer, B.t.u./min.
- ΔH^M = heat of mixing, B.t.u./lb.
- ΔH_i = enthalpy difference of one part of a loop with sign corresponding to a clockwise path around the loop, B.t.u./lb.
- μ = Joule-Thomson coefficient, ° R./p.s.i.a.
- ϕ = isothermal throttling coefficient, B.t.u./p.s.i.a.-lb.
- ∂ = partial derivative operator
- Σ = arithmetic summation operation
- $\hat{}$ = integral-average value

LITERATURE CITED

(1) Akers, W.W., Burns, J.F., Fairchild, W.R., *Ind. Eng. Chem.* **46**, 2531 (1954).
(2) Benedict, M., Webb, G.B., Rubin, L.C., *J. Chem. Phys.* **8**, 334 (1940).
(3) *Ibid.*, **10**, 747 (1942).
(4) Budenholzer, R.A., Botkin, D.F., Sage, B.H., Lacey, W.N., *Ind. Eng. Chem.* **34**, 878 (1942).
(5) Colwell, J.H., Gill, E.K., Morrison, J.A., *J. Chem. Phys.* **39**, 635 (1963).
(6) Cutler, A.J.B., Morrison, J.A., *Trans. Faraday Soc.* **61**, 429 (1965).
(7) Dillard, D.D., M.S. thesis, Oklahoma State University, 1966.
(8) Dittmar, P., Schultz, F., Strese, G., *Chem.-Ing. Tech.* **34**, 437 (1962).
(9) Douslin, D.R., Harrison, R.H., Moore, R.T., McCullough, J.P., J. CHEM. ENG. DATA **9**, 358 (1964).
(10) Edmister, W.C., Yarborough, L., *A.I.Ch.E. J.* **9**, 240 (1963).
(11) Ernst, G., Dr. Ing. dissertation, Universität Karlsruhe, Germany, 1967.
(12) Faulkner, R.C., Jr., Ph.D. thesis, University of Michigan, 1959.
(13) Frank, A., Clusius, K., *Z. physik. Chem.* **B36**, 291 (1937).
(14) Head, J.F., Ph.D. thesis, University of London, 1960.
(15) Helgeson, N.L., Sage, B.H., J. CHEM. ENG. DATA **12**, 47 (1967).
(16) Huang, E.T.S., Swift, G.W., Kurata, F., *A.I.Ch.E. J.* **13**, 846 (1967).
(17) Huff, J.A., Reed, T.M., III, J. CHEM. ENG. DATA **8**, 306 (1963).
(18) Jones, M.L., Jr., Ph.D. thesis, University of Michigan, 1961.
(19) Jones, M.L., Jr., Mage, D.T., Faulkner, R.C., Jr., Katz, D.L., *Chem. Eng. Progr. Symp. Ser.* **59** (44), 52 (1963).
(20) Kemp, J.D., Egan, C.J., *J. Am. Chem. Soc.* **60**, 1521 (1938).
(21) Kuloor, N.R., Newitt, D.M., Bateman, J.S., "Thermodynamic Functions of Gases," F. Din, Ed., Vol. **2**, p. 115, Butterworths, London, 1956.
(22) Manker, E.A., Ph.D. thesis, University of Michigan, 1964.

(23) Manker, E.A., Mage, D.T., Mather, A.E., Powers, J.E., Katz, D.L., *Proc. Ann. Conv., Natl. Gas Process. Assoc., Tech. Papers* **43**, 3 (1964).
(24) Manker, E.A., Mather, A.E., Bhirud, V., Powers, J.E., unpublished manuscript.
(25) Mather, A.E., Ph.D. thesis, University of Michigan, 1967.
(26) Mather, A.E., Katz, D.L., Powers, J.E., *Trans. Faraday Soc.* **64**, 2939 (1968).
(27) Mather, A.E., Powers, J.E., Katz, D.L., *Proc. Ann. Conv., Nat. Gas. Process. Assoc., Tech. Papers* **44**, 3 (1965).
(28) Mather, A.E., Powers, J.E., Katz, D.L., Thermodynamik-Symposium, Kl. Schäfer, Ed., Heidelberg, Germany, September 1967, p. I, 6, 1.
(29) Mather, A.E., Powers, J.E., Katz, D.L., *A.I.Ch.E. J.* **15**, 111 (1969).
(30) Mather, A.E., Yesavage, V.F., Katz, D.L., Powers, J.E., *Proc. Ann. Conv. Natl. Gas Process. Assoc., Tech. Papers* **46**, 8 (1967).
(31) Mather, A.E., Yesavage, V.F., Powers, J.E., Katz, D.L., *Ibid.*, **45**, 12 (1966).
(32) *Ibid.*, **46**, 3 (1967).
(33) Montgomery, J.B., DeVries, T., *J. Am. Chem. Soc.* **64**, 2372 (1942).
(34) Powers, J.F., Manker, E.A., Mather, A.E., Yesavage, V.F., AIChE Meeting, Cleveland, Ohio, May 4, 1968.
(35) Price, A.R., Kobayashi, R., J. CHEM. ENG. DATA **4**, 40 (1959).
(36) Reamer, H.H., Sage, B.H., Lacey, W.N., *Ind. Eng. Chem.* **42**, 534, 1258 (1950).
(37) Roebuck, J.R., *Phys. Rev.* **2**, 299 (1913).
(38) Roof, J.G., Baron, J.D., J. CHEM. ENG. DATA **12**, 292 (1967).
(39) Rossini, F.D., *et al.*, "Selected Values of Physical and Thermodynamic Properties of Hydrocarbons and Related Compounds," Carnegie Press, Pittsburgh, Pa., 1953.
(40) Rutherford, W.M., *Soc. Petrol. Engrs. J.* **2**, 340 (1962).
(41) Sage, B.H., Kennedy, E.R., Lacey, W.N., *Ind. Eng. Chem.* **28**, 601 (1936).
(42) Sage, B.H., Lacey, W.N., Schaafsma, J.G., *Ibid.*, **26**, 214 (1934).
(43) Sahgal, P.N., Geist, J.M., Jambhekar, A., Wilson, G.M., *Intern. Advan. Cryogen. Eng.* **10**, 224 (1965).
(44) Tester, H.E., "Thermodynamic Functions of Gases," F. Din, Ed., p. 1, Vol. **3**, Butterworths, London, 1961.
(45) Vennix, A.J., Ph.D. thesis, Rice University, 1966.
(46) Vennix, A.J., Leland, T.W., Kobayashi, Riki, *J. Chem. Phys.*, in press.
(47) Yarborough, L., Edmister, W.C., *A.I.Ch.E. J.* **11**, 492 (1965).
(48) Yesavage, V.F., Ph.D. thesis, University of Michigan, 1968.
(49) Yesavage, V.F., Furtado, A.W., Powers, J.E., *Proc. Ann. Conv. Natl. Gas Process. Assoc., Tech. Papers* **47**, 3 (1968).
(50) Yesavage, V.F., Katz, D.L., Powers, J.E., "Fourth Symposium on Thermophysical Properties," ASME, New York, 1968.
(51) Yesavage, V.F., Katz, D.L., Powers, J.E., to be published in *A.I.Ch.E. J.*
(52) Yesavage, V.F., Katz, D.L., Powers, J.E., J. CHEM. ENG. DATA, in press.

RECEIVED for review March 27, 1968. Accepted January 3, 1969. Research financed primarily with funds administered by the Thermodynamics Advisory Committee, Natural Gas Processors Association.

Molecular Diffusion Coefficients for the Triethylene Glycol–Water System

F. E. MERLISS[1] and C. P. COLVER
The University of Oklahoma, Norman, Okla. 73069

Molecular diffusion coefficients for the triethylene glycol–water system have been determined as a function of composition at 30°, 45°, and 65° C. The diffusion coefficients were determined from photographically recorded interferograms made at various time intervals during diffusion experiments and compared to a number of frequently used correlations.

THEORY of molecular diffusion for the gaseous state is relatively well developed in comparison to that for the liquid state. This, in part, results from the fact that the kinetic theory of the gaseous state is relatively well defined, while there is as yet no workable kinetic theory for the liquid state (*18*). Even so, predicted values for molecular diffusion coefficients in binary gaseous systems, determined by correlations developed from theoretical considerations, contain significant uncertainties and typically deviate from experimentally determined values by 5 to 10% at ambient conditions. Often greater deviations are encountered and for pressures in excess of 20 atm., at or below normal temperatures; these correlations fail to yield even reasonable estimates for the binary molecular diffusion coefficients (*25*). No single correlation of gaseous diffusion coefficients has been found to be superior over other correlations for all gaseous systems.

Since there is no workable kinetic theory of the liquid state, much less has been accomplished theoretically for the liquid state than for the gaseous state. Even for simple binary liquid systems, no widely applicable molecular diffusion coefficient correlations have been derived from theoretical considerations. However, a large number of correlations have been presented in the literature, ranging from purely empirical to semitheoretical in nature.

There is a great need for accurate binary molecular diffusion data for use in design work and for testing these correlations under a variety of conditions so that the quality of the correlations can be improved. The data presented herein were determined for use in the latter cause.

EXPERIMENTAL EQUIPMENT AND PROCEDURES

Experimental Equipment. The experimental equipment consisted of a birefringent interferometer, a constant temperature air bath with controls and recorder, a flowing junction cell, and a 35-mm. camera with auxiliary attachments.

Among the available methods for determining liquid diffusivities, those which employ interferometric techniques of analysis are considered capable of the greatest accuracy (*11, 14, 18*). Several interferometric techniques have been developed and used for this purpose.

After an analysis of the various types of interferometers,

[1] Present address: Textile Fibers Department, E. I. du Pont de Nemours & Co., Waynesboro, Va. 22980